Measurements of Elastic ρ- and φ-Meson Photoproduction Cross Sections on Protons from 30 to 180 GeV

R. M. Egloff, P. J. Davis, G. J. Luste, J. F. Martin, and J. D. Prentice
University of Toronto, Toronto, Ontario M5S1A7, Canada

and

D. O. Caldwell, J. P. Cumalat,[a] A. M. Eisner, A. Lu, R. J. Morrison, and S. J. Yellin
University of California, Santa Barbara, California 93106

and

T. Nash
Fermi National Accelerator Laboratory, Batavia, Illinois 60510
(Received 17 May 1979)

The elastic photoproduction cross sections for ρ and φ mesons from protons have been measured from 30 to 180 GeV. The energy dependences agree well with predictions made by using vector-meson dominance and an additive quark model. The ρ cross section is approximately constant with energy while the φ cross section rises from 0.5 to 0.7 μb with increasing energy.

In this paper we present results on the elastic photoproduction of ρ and φ mesons on protons, $\gamma p \to \rho^0 p$ and $\gamma p \to \varphi p$. The decay modes we observed were $\rho^0 \to \pi^+\pi^-$ and $\varphi \to K^+K^-$. The data were taken during the photon total-cross-section experiment[1] at the Tagged Photon Laboratory of Fermilab.

A schematic diagram of the apparatus is shown in Fig. 1. The hydrogen target is 1 m long and is surrounded by four scintillation recoil counters. The detectors S1 and S2 are multilayer lead-iron-scintillation counters; S3 and K are iron-scintillator hadrometers; G2 and G3 are lead-glass shower-counter arrays; and C and D are lead-scintillator shower detectors. In front of the G3 lead-glass array are six multiwire proportional chambers (MWPC's). More details on the detection apparatus can be found in Ref. 1.

Since the apparatus did not have a magnet or a Cherenkov counter, we were unable to measure mass spectra directly or to discriminate between pions and kaons for ρ^0- and φ-meson production. However, our full coverage of the forward hemisphere in the γp center-of-mass frame allowed us to select events with exactly two tracks, and no extra particles in S1, S2, S3, or G3. The opening angle multiplied by the two-track energy (assumed equal to the tagged-photon energy) provided an excellent substitute for the actual invariant mass, in that the ρ^0 and φ decays show up as two distinct peaks.

Consider now the elastic production of a short-lived meson, mass M and energy E (we neglect the recoil kinetic energy), which decays into two particles of mass $m \neq 0$. For $E \gg M$, the track separation, Δ, can be written to an excellent approximation as

$$\Delta = \frac{4Z \sin\theta[(\frac{1}{2}M)^2 - m^2]^{1/2}}{E[\sin^2\theta + (2m/M)^2\cos^2\theta]}, \quad (1)$$

where θ is the decay angle in the rest frame of M, and Z is the distance from the target to the position where Δ is measured.

When Eq. (1) is evaluated for the decay $\varphi \to K^+K^-$,

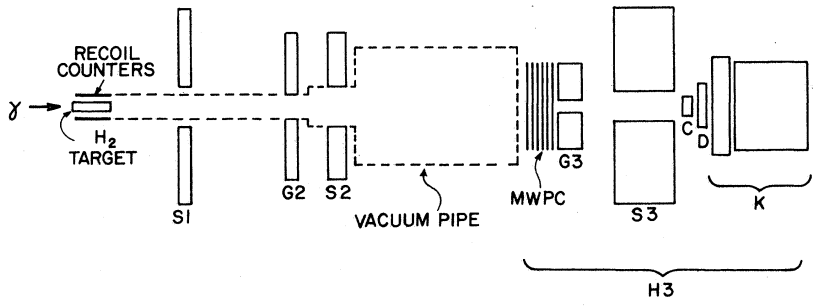

FIG. 1. Schematic diagram of apparatus.

the maximum track separation is $\Delta\varphi_{max} = 0.509Z/E$, whereas nearly all ρ^0 decays at $M = M_\rho$ (770) have $\Delta \geq 1.432Z/E$ (the value for $\theta = 90°$). From Eq. (1) we note that the distribution of $E\Delta$, or, more conveniently, $R \equiv \Delta/\Delta\varphi_{max}$ is independent of E. This makes it possible to plot a combined R spectrum for the entire tagging range ($E = 45$ to 92% of the electron beam energy, E_0).

Only events which satisfied certain criteria were included in the R distribution. An event was considered an elastic candidate if the event had exactly two tracks in the MWPC's and if more than 35% of the tagged-photon energy, E_γ, was contained in H3 (see Fig. 1). Next, all signals in G3 were required to be associated with tracks, and the upstream detectors, S1, S2, and G2, were used as veto counters. Finally, electromagnetic pairs were excluded by requiring the energy in G3 and C to be less than 60% of E_γ. The R distribution for $E_0 = 90$ GeV is shown in Fig. 2(a).

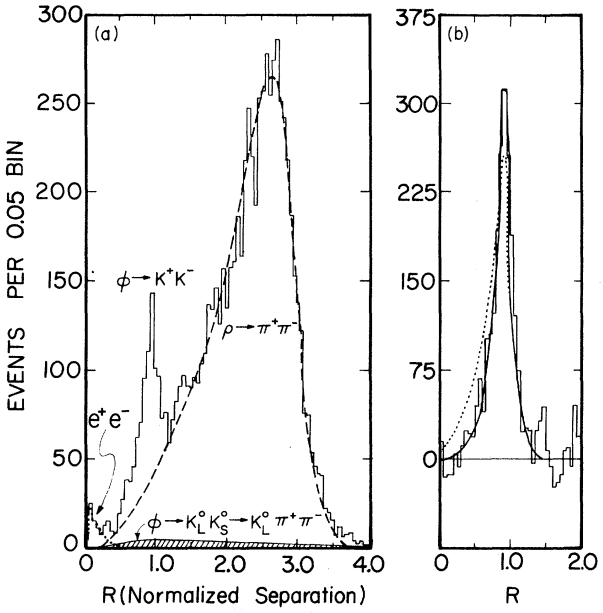

FIG. 2. (a) R distribution for $E_0 = 90$ GeV data. The various curves are explained in the text. (b) The φ signal above background summed over all data points.

In order to extract ρ^0 and φ yields from data plots like Fig. 2(a), a Monte Carlo program was used to produce expected R distributions. Under the assumption of s-channel helicity conservation[2] and hence, a $\sin^2\theta$ decay distribution, R spectra for ρ^0 and φ decays were generated with use of the known photon spectrum. The Monte Carlo calculation folded in the ρ mass shape, geometrical acceptance, target length, beam size, and resolution in photon energy and in Δ. Cross sections are assumed to vary with t (t is the square of the four-momentum transfer) like e^{bt} with $b(\rho) = 8.5$ GeV^{-2} and $b(\varphi) = 6.5$ GeV^{-2}. Results were insensitive to uncertainties in these numbers aside from a weak dependence of the ρ acceptance on $b(\rho)$.

The ρ mass spectrum requires further discussion. We have used the Söding parametrization[3,4] of a ρ interfering with a nonresonant background:

$$\frac{dN}{dM} = \frac{C_0 M M_\rho \Gamma}{(M^2 - M_\rho{}^2)^2 + M_\rho{}^2\Gamma^2}\left\{1 + C_1\left(\frac{M_\rho{}^2}{M^2} - 1\right) + C_2\left(\frac{M_\rho{}^2}{M^2} - 1\right)^2\right\}, \quad (2)$$

with $M_\rho = 0.773$ GeV and a mass-dependent width[5]

$$\Gamma = \left[\frac{q(M)}{q(M_\rho)}\right]^3 \frac{2\Gamma_0}{1 + [q(M)/q(M_\rho)]^2}. \quad (3)$$

Here $\Gamma_0 = 0.150$ GeV, and $q(M)$ is the magnitude of the three-momentum in the π-π center-of-mass frame. The ρ^0 yield is then defined to equal $(\pi/2)C_0$.[4]

Two additional processes have been included. The decay $\varphi \to K_L{}^0 K_S{}^0 \to K_L{}^0 \pi^+\pi^-$ has been computed to contribute less than 1% to the ρ; it is shown in Fig. 2(a). There is also a small low-R contribution surviving our cuts from Bethe-Heitler e^+e^- pairs in which one member has interacted hadronically in C or G3. Their R dependence was obtained from noninteracting pairs, but the normalization (N_{ee}) left free. By use of the R spectra for all contributions, five-parameter fits were done to determine C_0, C_1, C_2, the φ yield, and N_{ee}. Good fits were obtained for all data points, giving average C_1 and C_2 values of 3.0 ± 0.7 and 2.0 ± 0.5. The total ρ and e^+e^- contributions for the 90-GeV electron energy setting are drawn in Fig. 2(a). Figure 2(b) shows the φ data (summed over all data points) with all other processes subtracted; also shown are predicted R spectra assuming s-channel helicity conservation (solid line) and, for comparison, isotropic decay (dotted line).

Corrections to the ρ^0 and φ yields were applied for geometric acceptance (the acceptance determined by the Monte Carlo program averaged 60% for the ρ and 96% for the φ), two-track recon-

TABLE I. The cross section with statistical uncertainties for $\gamma p \to \rho^0 p$ and $\gamma p \to \varphi p$.

E_0 (GeV)	E_γ (GeV)	$\sigma_{\gamma \to \rho^0} \pm \Delta\sigma$ (μb)	$\sigma_{\gamma \to \varphi} \pm \Delta\sigma$ (μb)
60	35 ± 5	8.84 ± 0.44	0.506 ± .090
60[a]	42 ± 12	10.68 ± 0.67	0.568 ± .091
60	47 ± 7	9.90 ± 0.49	0.546 ± .089
90	53 ± 7	9.50 ± 0.56	0.625 ± .063
90	71 ± 11	9.82 ± 0.56	0.646 ± .065
135	79 ± 11	8.24 ± 0.47	0.648 ± .052
135	106 ± 16	9.22 ± 0.52	0.661 ± .053
200	117 ± 17	8.59 ± 0.49	0.630 ± .101
200	157 ± 23	9.75 ± 0.56	0.740 ± .092

[a]Data taken at a modified geometry.

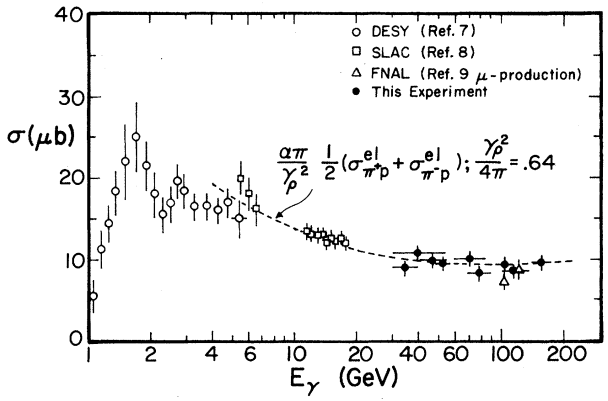

FIG. 3. Energy dependence of the ρ^0 photoproduction cross section.

struction inefficiency (9%), inelastic π or K interactions between production and chambers (15% and 11%), decays in flight (averaging 1% and 7%), events lost by analysis cuts (4% and 4%), and the φ branching ratio to K^+K^- (46.6%).

We also corrected for contamination from inelastic events involving target dissociation with no downstream products. Elastic and inelastic events could be statistically distinguished by their different probabilities for firing n of the four recoil counters. Diffractive events have $n \leq 1$, usually $n=0$, with probabilities computable from range-energy relations. Inelastic events almost always have $n \geq 1$, usually $n>1$. Probabilities were estimated by a simple Poisson model which agrees with hadronic studies of target dissociation,[6] but our results are not very sensitive to details of the model. The inelastic events eliminated amounted to 13% for the ρ^0, and 18% for the φ.

The resulting cross sections are presented in Table I and are shown in Figs. 3 and 4, along with results of previous experiments.[2,7-12] The quoted errors are statistical and include uncertainties due to background subtraction. The total energy-independent systematic uncertainties are estimated to be less than 5%. For the ρ there is an additional 5% systematic uncertainty due to geometrical acceptance. The curve in Fig. 4 is from a parametrization of all the data[13] and shows a rising cross section with increasing energy.

In vector-meson dominance (VMD) models, the photoproduction of a vector meson, V, is related to Vp scattering. The Vp scattering can in turn be related by additive quark-model relations to measured hadron processes. If we assume that the VMD and quark-model relations apply to amplitudes at fixed s and t, then one can "predict" photoproduction cross sections in terms of hadronic elastic scattering cross sections:

$$\frac{d\sigma}{dt}(\gamma p \to \rho^0 p) = \frac{e^2}{4\gamma_\rho{}^2}\left(\frac{p_\pi{}^*}{2p_\gamma{}^*}\left\{\left[\frac{d\sigma}{dt}(\pi^+ p)\right]^{1/2}+\left[\frac{d\sigma}{dt}(\pi^- p)\right]^{1/2}\right\}\right)^2, \tag{4a}$$

$$\frac{d\sigma}{dt}(\gamma p \to \varphi p) = \frac{e^2}{4\gamma_\varphi{}^2}\frac{1}{(p_\gamma{}^*)^2}\left(p_K{}^*\left\{\left[\frac{d\sigma}{dt}(K^+ p)\right]^{1/2}+\left[\frac{d\sigma}{dt}(K^- p)\right]^{1/2}\right\}-p_\pi{}^*\left[\frac{d\sigma}{dt}(\pi^- p)\right]^{1/2}\right)^2, \tag{4b}$$

where $p_x{}^*$ is the three-momentum of x in the xp center-of-mass frame, and everything is to be evaluated at the same s. For our purposes the integral of (4a) is well approximated by

$$\sigma(\gamma p \to \rho^0 p) \simeq \frac{e^2}{4\gamma_\rho{}^2}\tfrac{1}{2}[\sigma(\pi^+ p \to \pi^+ p)+\sigma(\pi^- p \to \pi^- p)]. \tag{5}$$

This formula is plotted in Fig. 3, with use of smoothed πp measurements[14-16] and $\gamma_\rho{}^2/4\pi = 0.64$,[17] and is seen to represent the photoproduction data well.

For the φ, we have used forward hadron-beam data[14-16] and assumed an e^{bt} form for the photoproduction cross section with $b(s) = 4.66 \pm 0.38 \ln s$.[12] The resulting predictions, normalized to our data, are shown in Fig. 5 along with the curve from Fig. 4. The energy dependence is similar; the measured

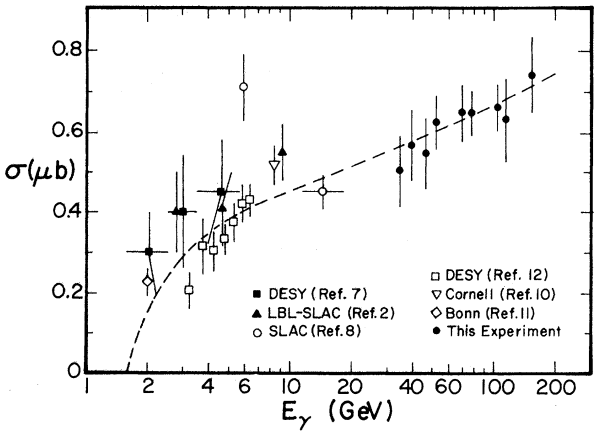

FIG. 4. Energy dependence of the φ photoproduction cross section. Dashed line is a parametrization of the cross section.

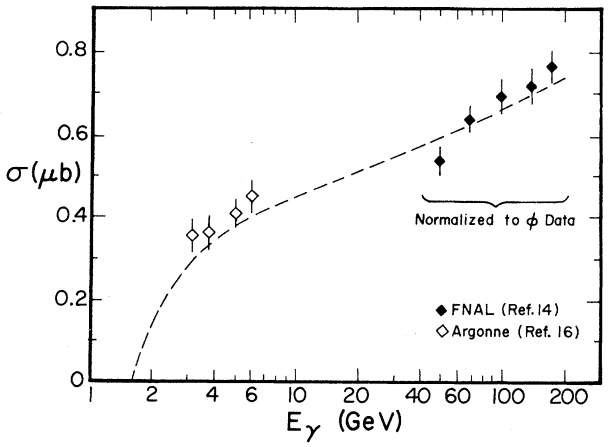

FIG. 5. VMD–quark-model cross section normalized to the φ data of this experiment. The curve is the same as in Fig. 4.

value of $\gamma_\varphi^2/4\pi = 4.7 \pm 0.3$ resulting from the normalization is consistent with the value of 5.5 ± 2.4 obtained from a photoproduction experiment[17] on complex nuclei. A value of 2.83 ± 0.2 is obtained from colliding-beam measurements.[17] We conclude that the energy dependence of the φp elastic cross section extracted from hadronic data (Using the quark model) and from photoproduction (using VMD) are in agreement.

We gratefully acknowledge support from the Fermilab staff, especially the Proton and Physics Departments and the Hydrogen Target group. We thank F. Murphy who participated in the early stages of the experiment. We also thank our technical support personnel, including M. Armstrong, D. Briggs, Y. Chan, A. Kiang, H. Nickel, D. Simmen, and R. Stuber, and students, J. Gallet and C. Lauer. Valuable assistance was provided by M. Franklin and M. G. Donnelly, and also by A. Belousov and B. Govorkov of the Lebedev Physical Institute. This research was supported in part by the U. S. Department of Energy, and by the National Research Council of Canada through the Institute of Particle Physics of Canada.

[a]Present address: Fermi National Accelerator Laboratory, Batavia, Ill. 60510.

[1]D. O. Caldwell *et al.*, Phys. Rev. Lett. 40, 1222 (1978); J. P. Cumalat, thesis, University of California, Santa Barbara, 1977 (unpublished).
[2]J. Ballam *et al.*, Phys. Rev. D 7, 3150 (1973).
[3]P. Söding, Phys. Lett. 19, 702 (1965).
[4]R. Spital and D. R. Yennie, Phys. Rev. D 9, 126 (1974).
[5]J. D. Jackson, Nuovo Cimento, 34, 1644 (1964).
[6]J. Whitmore, Phys. Rep. 10, 273 (1974).
[7]Aachen-Berlin-Bonn-Hamburg-Heidelberg-München Collaboration, Phys. Rev. 175, 1669 (1968).
[8]R. Anderson *et al.*, Phys. Rev. D 1, 27 (1970).
[9]W. R. Francis *et al.*, Phys. Rev. 38, 633 1977).
[10]C. Berger *et al.*, Phys. Lett. 39B, 659 (1972).
[11]H. J. Besch *et al.*, Nucl. Phys. B70, 257 (1974).
[12]H. J. Behrend *et al.*, Nucl. Phys. B144, 22 1978).
[13]The curve is given by $\sigma = (p_\varphi^*/p_\gamma^*)^2 (a + b/s^{1/2} + c \ln s)$ with $a = -0.10 \pm 0.33$, $b = 0.94 \pm 0.64$, $c = 0.14 \pm 0.06$, σ in μb and s in GeV^2.
[14]D. S. Ayres *et al.*, Phys. Rev. D 15, 3105 (1977).
[15]K. J. Foley *et al.*, Phys. Rev. Lett. 9, 425 (1963).
[16]I. Ambats *et al.*, Phys. Rev. D 9, 1179 (1974).
[17]D. W. G. S. Leith in *Electromagnetic Interactions of Hadrons*, edited by A. Donnachie and G. Shaw, (Plenum, New York, 1978).